

Effect of Air flow on Heat transfer within Dynamic Building Walls

Asst. Lect. Wisam K. Hussam
Educational Technology Department
University of Technology, Baghdad, Iraq

Abstract

In this work, an analytical model is presented to show the air leakage effect on the heat transfer within a permeable 120 mm thick, fiber glass wall. Both steady-state and steady periodic conditions are considered for the inner and the outer surfaces of the wall. Computer calculations are made to determine the temperature profiles and heat flux variations within the wall taking into consideration the infiltration and exfiltration of air. The effect of air flows on the heat transmission through the wall is studied and the thermal advantages of the circulating air through the building walls are analyzed.

The study is concentrating on the thermal performance of dynamic walls integrated in a whole building, as a function of the infiltration and exfiltration rates and the building thermal load. The results indicate that the dynamic walls can save energy of up to 20 percent of the total building thermal load.

الخلاصة

في هذا البحث تم عرض نموذج تحليلي لإظهار تأثير تسرب الهواء على انتقال الحرارة ضمن جدار نفاذ بسلك 120 ملم من الفايبركلاس باعتماد كل من الحالة المستتبة والمستتبة الدورية عند الأسطح الداخلية والخارجية للجدار. تم استخدام الحاسب الإلكتروني لإيجاد توزيع درجات الحرارة والفيض الحراري خلال الجدار مع الأخذ بنظر الاعتبار التسرب الداخلي والخارجي للهواء. إن تأثير جريان التيارات الهوائية على انتقال الحرارة خلال الجدار تمت دراستها وكذلك تم تحليل الفوائد الحرارية للهواء المداور خلال جدران البناية. الدراسة تركزت على الأداء الحراري للجدران الدينامكية المتكاملة مع البناية كدالة إلى معدل التسرب الداخلي والخارجي للهواء وحمل البناية الحراري. النتائج تشير إلى إن الجدران الدينامكية يُمكنها توفير طاقة بحدود 20 بالمائة من الحمل الحراري الكلي للبناية.

1. Introduction

Heat loss/gain in buildings can be significantly affected by the amount of air flowing from outside to inside (infiltration) and from inside to outside (exfiltration). Currently the air leakage rates due to infiltration or exfiltration can be accurately predicted. However, the effect of these air flows on heat transfer in building envelopes has not been thoroughly analyzed. It has always been assumed that the air infiltration would increase the heating load of a building by the product of air flow rate times the enthalpy difference between inside and outside the building (or simply the temperature difference). The effects of air flow on heat transmission building envelopes are rarely taken into account.

Recent experimental and numerical studies have demonstrated that significant thermal coupling can occur between air leakage and insulation layers, thereby modifying the heat transmission in building envelopes. A number of researchers Berlad et. al. ^[1], Wolf ^[2], Bankvall ^[3], Lecompte ^[4], Buchanan and Sherman ^[5] have shown that convective air flow degrades the effective thermal resistance of air-permeable insulations. This R-value degradation occurs when outside air moves through and/or around the insulation within the wall cavity, and returns to outdoor without reaching the conditioned space. Powell et. al. ^[6] provided a literature review summarizing the findings on the air movement influence on the effective thermal resistance of porous insulations under various conditions.

When air flows from outside into a conditioned space, the heating load due to the combined conduction and convection heat transfer can be lower than the heating load due to transmission losses added to the normal infiltration losses. This reduction in total heating load is a consequence of the thermal coupling between conduction and convection heat transfer.

Indeed, air infiltrating a building recovers heat from the building envelope. Using a computer simulation code, Kohonen et. al. ^[7] found that the effect of the conduction/infiltration thermal interaction was a reduction of 15 percent in total heating load. Similar results have been found by Claridge et. al. ^[8] using a test cell to measure the energy impact of air infiltration.

Kohonen and Ojanen ^[9] have demonstrated the energy savings potential of dynamic insulation systems in which air is circulated through the building envelope from outdoors to indoors to provide ventilation. Bailey ^[10] found that the energy savings of dynamic insulations can reach 14 percent during a heating period.

This paper presents an analytical model to characterize and evaluate the air leakage effects on the heat conduction within a one-layered wall. Both steady-states and steady-periodic conditions are considered in the inner and outer surfaces of the wall. The temperature profiles within the wall as well as the heat flux along the inner and outer wall surfaces are analyzed to show the effect of air flow on heat transmission through buildings envelope. Finally, the thermal efficiency of a dynamic wall is analyzed for various infiltration rates and building thermal loads under steady-state and steady periodic conditions.

2. Mathematical Model

The temperature distribution within a wall subject to air infiltration determined by applying the first law of thermodynamics. For the control volume of finite size dx as shown in Fig.(1), the first law of thermodynamics requires that:

$$\left[\begin{array}{l} \text{the rate of energy} \\ \text{accumulation in} \\ \text{the control volume} \end{array} \right] = \left[\begin{array}{l} \text{the net heat} \\ \text{transfer by} \\ \text{air} \end{array} \right] + \left[\begin{array}{l} \text{the net heat} \\ \text{transfer by} \\ \text{conduction} \end{array} \right]$$

$$\delta q = (q_{a,x} - q_{a,x+dx}) + (q_{c,x} - q_{c,x+dx}) \dots\dots\dots (1)$$

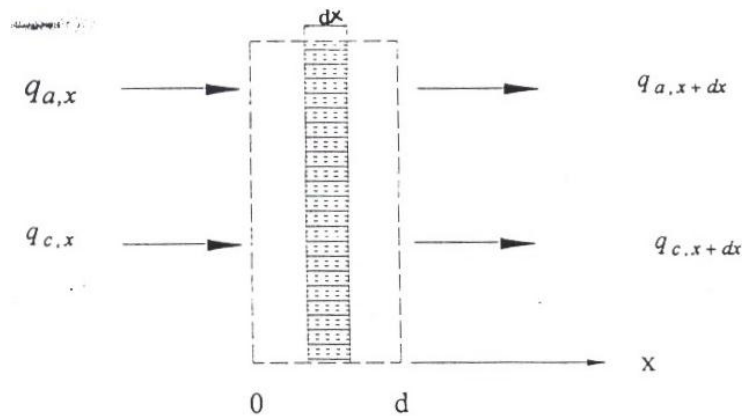


Figure (1) Control volume element of a wall

Since both solid material and air are present in the control volume, dx , the rate of energy accumulation in dx is:

$$\delta q = \frac{\partial}{\partial t} ([(1 - \epsilon)\rho_w c_w + \epsilon \rho_f c_f] T) dx \dots\dots\dots (2)$$

By defining $(\rho c)_{wf}$ as $(1 - \epsilon)\rho_w c_w + \epsilon \rho_f c_f$, Equation (2) can be re-written as follows:

$$\delta q = (\rho c)_{wf} \frac{\partial T}{\partial t} dx \dots\dots\dots (3)$$

The net heat transfer by air infiltration is:

$$q_{a,x} - q_{a,x+dx} = (\rho_f U_f c_f T) - [\rho_f U_f c_f T + \frac{\partial}{\partial x} (\rho_f U_f c_f T) dx] \dots\dots\dots (4)$$

Assuming that the air velocity U_f does not change across the wall, it follows that:

$$q_{a,x} - q_{a,x+dx} = -\rho_f U_f c_f \frac{\partial T}{\partial x} dx \dots\dots\dots (5)$$

The net heat transfer by conduction is determined using Fourier's law:

$$q_{a,x} - q_{a,x+dx} = -k_w \frac{\partial T}{\partial x} dx - [(-k_w \frac{\partial T}{\partial x} dx - \frac{\partial}{\partial x} (k_w \frac{\partial T}{\partial x} dx))] \dots\dots\dots (6)$$

The thermal conductivity of wall solids material, k_w , does not change significantly for the temperature range encountered in buildings:

$$q_{a,x} - q_{a,x+dx} = k_w \frac{\partial^2 T}{\partial x^2} dx \dots\dots\dots (7)$$

Substituting of equations (3), (5), and (7) into equation (1) yields to:

$$k_w \frac{\partial^2 T}{\partial x^2} - \rho_f U_f c_f \frac{\partial T}{\partial x} = (\rho c)_w \frac{\partial T}{\partial t} \dots\dots\dots (8)$$

2-1 Model Description

Figure (2) shows a one-layered wall with homogeneous thermal properties subject both to heat conduction due to the temperature difference between inside, T_i and outside, T_e , and to air leakage with a velocity, U_f . Assuming one-dimensional mass and heat flows. The temperature $T(x,t)$ within the wall is governed by the equation (8). Within the wall, the material properties and the air velocity are assumed to be constant. This assumption is justified by the small magnitude of the temperature variation in building walls. Furthermore, and since the air flow through building walls is laminar, the capacity to conduct heat is independent of the air velocity.

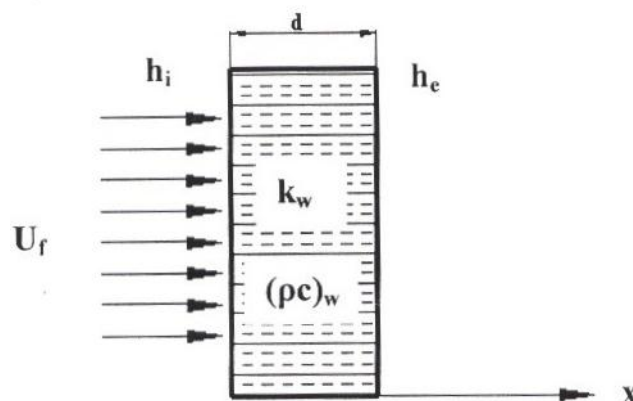


Figure (2) Wall model for the thermal coupling between heat transmission and air flow

$T(x, t)$ is assumed to represent the temperature of both the air and the wall material at the location x and time t . This assumption is routinely made in modeling porous media and is based on the local thermodynamic equilibrium (LTE) concept. The LTE assumption has been substantiated by Vafai and Sozen^[11] using an elaborate numerical model. They found that for typical thermo physical and infiltration data for porous insulation, the LTE assumption leads to less than a one percent error.

In Eq.(8) the velocity U_f positive in the positive x -direction (see Fig.(2)), that is when air flows from the conditioned space to outdoors (i.e., air exfiltration). When air flows from the outdoors to a conditioned space (i.e., infiltration), U_f is negative. The boundary conditions for Equation (8) are:

$$-k_w \frac{\partial T}{\partial x}(x, t) = h_i (T_i - T) \dots\dots\dots (9)$$

$$-k_w \frac{\partial T}{\partial x}(d, t) = h_e (T - T_e) \dots\dots\dots (10)$$

h_i and h_e are the film coefficients for convection heat transfer at the inner and outer wall surfaces, respectively. T_i is the indoor temperature and T_e is the sol-air temperature at the outside wall surface. In the absence of solar radiation, T_e reduces to the outdoor temperature. T_i and T_e are assumed to vary sinusoidally with time:

$$T_i = T_{i,m} + T_{i,a} \cos(\omega t + \phi_i) = T_{i,m} + \text{Re}(J_{i,a} e^{j\omega t})$$

and,

$$T_e = T_{e,m} + T_{e,a} \cos(\omega t + \phi_e) = T_{e,m} + \text{Re}(J_{e,a} e^{j\omega t})$$

while $J_{i,a}$ and $J_{e,a}$ are complex temperature amplitudes define as:

$$J_{i,a} = T_{i,a} e^{j\phi_i}$$

and,

$$J_{e,a} = T_{e,a} e^{j\phi_e}$$

Using the complex temperature technique it can be shown that the solution of equation (8), subject to the boundary conditions (9) and (10), is of the form

$$T(x, t) = T_m + \text{Re}(J_a e^{j\omega t}) \dots\dots\dots (11)$$

with J_a a complex temperature amplitude solution of :

$$j(\rho c)_{wf} \omega J + (\rho c)_f U_f \frac{\partial J}{\partial x} = k_w \frac{d^2 J}{da^2} \dots\dots\dots (12)$$

and,

$$\theta(\xi) = e^{Pe\xi/2} \frac{(2B_i B_e + Pe B_i) \sinh \beta(1 - \xi) + 2\beta B_i \cosh \beta(1 - \xi)}{[2B_i B_e - Pe^2/2 + 2\beta^2 + Pe(B_i - B_e)] \sinh \beta + 2\beta(B_i + B_e) \cosh \beta} \dots\dots (13)$$

$$-k_w \frac{\partial J}{\partial x}(d) = h_e (J - J_{e,a}) \dots\dots\dots (14)$$

T_m(x) is the mean temperature and is the solution of:

$$(\rho c)_f U_f \frac{\partial T_m}{\partial x} = k_w \frac{\partial^2 T_m}{\partial x^2} \dots\dots\dots (15)$$

and,

$$-k_w \frac{\partial T_m}{\partial x}(0) = h_i (T_{i,m} - T_m) \dots\dots\dots (16)$$

$$-k_w \frac{\partial T_m}{\partial x}(d) = h_i (T_m - T_{e,m}) \dots\dots\dots (17)$$

Note that T_m(x) can be obtained from the solution of equations (12)-(14) by setting ω to zero and replacing T_{i,a} and T_{e,a} by T_{i,m}, and T_{e,m} respectively. Therefore, only the solution J(x) needed to solve equation (8) with the boundary conditions (9) and (10).

Before obtaining the expression of J(x), let us normalized equations (12), (13), and (14). For this purpose we define the non-dimensional parameters:

$$\theta = \frac{J - J_{e,a}}{J_{i,a} - J_{e,a}} ; \quad \delta^2 = \frac{j(\rho c)_{wf} \omega d^2}{K_w}$$

$$Bi = \frac{h_i d}{K_w} ; \quad Be = \frac{h_e d}{K_w}$$

$$\xi = \frac{x}{d} ; \quad Pe = \frac{(\rho c)_f U_f d}{K_w}$$

B_i and B_e represent the Biot number at the inner and outer surface of the wall. Pe is pecllet number of the air flow. For a layer of mineral fiberglass (K_w= 0.04W/m.K) of thickness d = 120 mm, typical values of Biot numbers B_i and B_e are 100 and 25, respectively. The Peclet number for the same layer of fiberglass ranges from 1 to 10 as the air velocity varies from 1 m/s to 10 m/s.

Using the parameters defined above, equations (12), (13), and equation (14) becomes:

$$\delta^2 \theta + Pe \frac{d\theta}{d\xi} = \frac{d^2\theta}{d\xi^2} \dots\dots\dots (18)$$

$$\frac{d\theta}{d\xi}(0) = -B_i(1 - \theta) \dots\dots\dots (19)$$

$$\frac{d\theta}{d\xi}(d) = -B_e \theta \dots\dots\dots (20)$$

The solution of the above equations can be expressed as:

$$\theta(\xi) = e^{0.5Pe\xi} \frac{(2B_iB_e + PeB_i) \sinh \beta(1 - \xi) + 2\beta B_i \cosh \beta(1 - \xi)}{[2B_iB_e - 0.5Pe^2 + 2\beta^2 + Pe(B_i - B_e)] \sinh \beta + 2\beta(B_i + B_e) \cosh \beta} \dots\dots\dots (21)$$

where, $\beta = \sqrt{\delta^2 + 0.25Pe^2}$

In the no-flow conditions, that is, when no air is flowing through the wall, the normalized complex temperature amplitude is obtained from equation (21) by setting Peclet number to zero.

$$\theta(\xi) = \frac{2B_iB_e \sinh \beta(1 - \xi) + 2\beta B_i \cosh \beta(1 - \xi)}{[2B_iB_e + 2\delta^2] \sinh \delta + 2\delta(B_i + B_e) \cosh \delta} \dots\dots\dots (22)$$

For steady-state conditions, the temperature is independent of time, the temperature profile within the wall is obtained from equation (21) by setting ($\omega = 0$ and thus $\delta = 0$).

$$\theta(\xi) = e^{0.5Pe\xi} \frac{(2B_iB_e + PeB_i) \sinh \frac{Pe}{2}(1 - \xi) + Pe B_i \cosh \frac{Pe}{2}(1 - \xi)}{[2B_iB_e + Pe(B_i - B_e)] \sinh \frac{Pe}{2} + Pe(B_i + B_e) \cosh \frac{Pe}{2}} \dots\dots\dots (23)$$

In the case of air infiltration, the temperature within the wall can be obtained from equation (21) by replacing Pe by -Pe.

2-2 Heat Flux

The conductive heat flux I(x, t) across a surface (x) of the wall varies sinusoidally with time and can be expressed as:

$$I(x, t) = -K_w \frac{\partial T}{\partial x}(x, t) = I_m(x) + Re(q_a e^{j\omega t}) \dots\dots\dots (24)$$

With $Im(x)$ and q_a are , respectively, the mean and the complex amplitude of conductive heat flux across the surface (x). The conductive heat flux complex amplitude q_a is related to the temperature complex amplitude as follows:

$$q_a(x) = -K_w \frac{dq_a}{dx}(x) \dots\dots\dots (25)$$

The conductive heat flux mean value $Im(x)$ can obtain from $q_a(x)$ by setting ω to zero. The conductive heat flux complex amplitude q_a can be normalized:

$$\psi(\xi) = -\frac{dq_a(x)}{K_w(J_{i,a} - J_{e,a})} \dots\dots\dots (26)$$

The normalized complex amplitude of the conductive heat flux $\psi(\zeta)$ across a given surface ζ of the wall is defined as the derivative of normalized temperature $\theta(\zeta)$ as expressed in equation (21) (i.e., $\psi(\xi) = - d\theta/d\xi$)

$$\psi(\xi) = \frac{Pe}{2} e^{0.5Pe\xi\beta} \frac{(2B_i B_e + PeB_i) \cosh\beta(1-\xi) + 2\beta B_i \sinh \beta(1-\xi)}{[2B_i B_e - 0.5Pe^2 + 2\beta^2 + Pe(B_i - B_e)] \sinh \beta + 2\beta(B_i + B_e) \cosh\beta} \dots\dots (27)$$

In the no-flow conditions ($Pe=0$), the normalized complex conductive heat flux amplitude is reduced to:

$$\psi(\xi) = -\delta \frac{2B_i B_e \cosh\delta(1-\xi) + 2\delta B_i \sinh \delta(1-\xi)}{[2B_i B_e + 2\delta^2] \sinh \delta + 2\delta(B_i + B_e) \cosh\delta} \dots\dots\dots (28)$$

For steady-state conditions, the normalized conductive heat flux, $\psi(\zeta)$ at a given surface ζ of the wall can be deduced from equation (27) by setting ($\delta = 0$ and thus $\beta = Pe/2$).

$$\theta(\xi) = Pe B_i B_e \frac{e^{Pe(\xi-1/2)}}{[2B_i B_e - Pe(B_i - B_e)] \sinh Pe/2 + 2\beta(B_i + B_e) \cosh Pe/2}$$

2-3 Thermal Efficiency of Dynamic Walls

Walls that are built so a controlled flow of air can be passed through the porous insulation in the wall have been termed "dynamic" walls. The construction of such wall is described by Timusk [12]. **Figure (3)** shows a simplified model of a building equipped with a dynamic wall. In the dynamic wall, air is forced to the inside through a porous insulation layer. As illustrated in **Fig.(3)**, air infiltrates the house either through the dynamic wall (U_f) or through other cracks ($U_f - U_{vent}$). The infiltration air is then exhausted to the outside through vents (U_{vent}). The infiltration air is then exhausted to the outside through vents (U_{vent}). The areas of the dynamic wall and of the vents are A_w and A_{vent} , respectively.

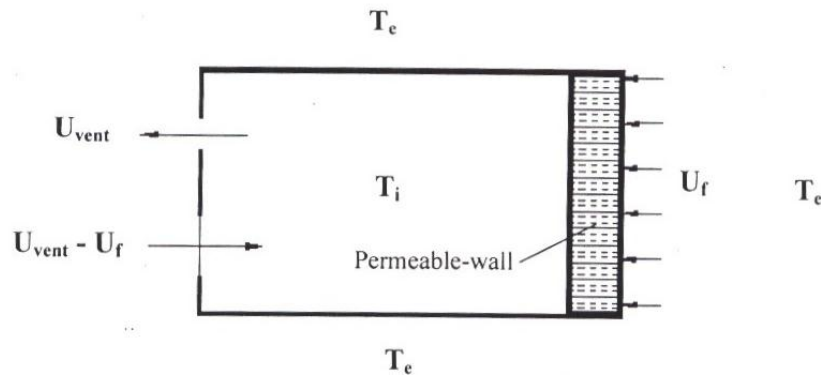


Figure (3) Section of simplified model for a dynamic wall integrated in a whole building

To determine the performance of the dynamic wall, the building thermal load is first estimated under no-flow conditions (i.e., no air flow through the dynamic wall)

$$E_s = Q_{cond,s}(0) + Q_{vent} + Q_{misc} \dots \dots \dots (29)$$

where:

$Q_{cond,s}(0)$: Conductive losses from dynamic wall calculated from equations (24) and (27)

($Q_{cond,s}(0) = A_w I_m(0)$) with A_w the area of the dynamic wall.

Q_{vent} : Heat loss due to ventilation ($Q_{vent} = (\rho c)_f U_{vent} A_{vent} [T_i - T_e]$)

Q_{misc} : Heat loss from source other than ventilation and dynamic wall, such as floor and ceiling wall.

Then, the building thermal load is calculated when the air is allowed to flow through the dynamic wall:

$$E_d = Q_{cond}(0) + Q_{vent} + Q_{misc} \dots \dots \dots (30)$$

where:

$Q_{cond}(0)$: is now estimated from equation (24) and (28).

Note that the air flow through the porous wall is typically induced by a fan. The fan energy use will be neglected to simplified analysis. The performance of the dynamic wall is defined as:

$$\eta_w = 1 - \frac{E_d}{E_s} \dots \dots \dots (31)$$

The efficiency η_w is a measure of the energy savings that the dynamic wall can achieve in percent of total building thermal load. A convenient way to characterize the building thermal load is to introduce the fractions C_{cond} , C_{vent} , C_{misc} as:

$$C_{\text{cond}} = \frac{Q_{\text{cond}}(0)}{E_s} \dots\dots\dots (32)$$

$$C_{\text{vent}} = \frac{Q_{\text{vent}}}{E_s} \dots\dots\dots (33)$$

$$C_{\text{cond}} = \frac{Q_{\text{misc}}}{E_s} \dots\dots\dots (34)$$

After arrangement, it can be shown that dynamic wall efficiency can expressed as:

$$\eta_w = C_{\text{cond}} \left(1 - \frac{Q_{\text{cond}}(0)}{Q_{\text{cond},s}(0)} \right) \dots\dots\dots (35)$$

The air flow rate forced through the dynamic wall is limited by the amount of air exhausted, i.e.,

$$(\rho c)_f A_w U_f \leq (\rho c)_f A_{\text{vent}} U_{\text{vent}}$$

Under steady-state conditions, the above limitation can be expresses as:

$$Pe = \frac{(\rho c)_f U_f d}{K_w} \leq \frac{(\rho c)_f U_{\text{vent}} U_{\text{vent}} (T_i - T_e)}{K_w A_w (T_i - T_e) / d} = \frac{Q_{\text{vent}}}{Q_s(0)} = \frac{C_{\text{vent}}}{C_{\text{cond}}}$$

or, since:

$$C_{\text{vent}} = 1 - C_{\text{cond}} - C_{\text{misc}} \leq 1 - C_{\text{cond}} \dots\dots\dots (36)$$

Thus,

$$Pe \leq \frac{(1 - C_{\text{cond}})}{C_{\text{cond}}} \dots\dots\dots (37)$$

3. Results and Discussion

Figure (4) shows normalized temperature profiles within a wall for varies Peclet numbers. As indicated, the temperature within the wall is deformed by the air leakage. This deformation depends on the amount and direction of the air flow. When no air flows, the temperature varies linearly within the wall. When air is exfiltrating, the temperature profile takes a convex shape. When air is infiltrating, the temperature profile has a concave shape. This change in temperature profile affects the heat loss due to conduction through the wall. In addition to the temperature profile deformation, the heat transfer by convection at the wall surfaces is increased by exfiltrating air, resulting in a decrease in the temperature of the inner

wall surface. When air is infiltrating, the heat transfer by convection is decreased and the temperature of the inner wall surface is increased.

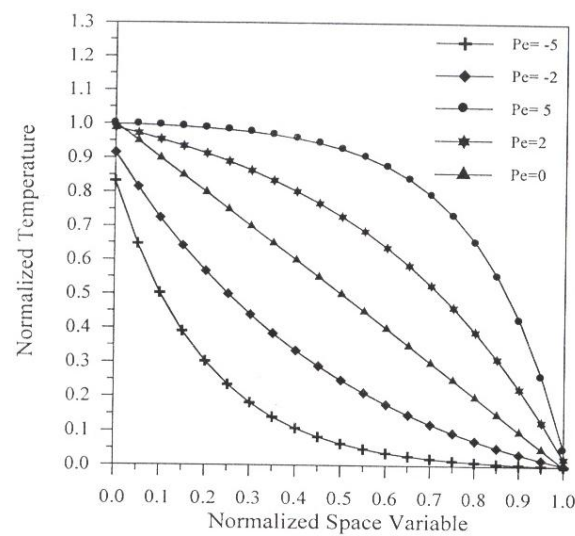


Figure (4) Normalized wall temperature profiles with convection under steady-state condition

Figure (5) illustrates the temperature profile within the wall when the outside temperature varies sinusoidally with time. The same deformation effect of the temperature profiles caused by infiltrating ($Pe = -5$) or exfiltrating air ($Pe = 5$) is again noticeable in the steady-periodic conditions. The effect of the air leakage is coupled with the mass effect of the wall to shape the temperature variations with time across the wall. In the no-flow conditions ($Pe = 0$), the temperature profile is almost linear, indicating that the thermal mass effect is not significant for the wall, because the low U-value and the small heat capacity of porous insulation.

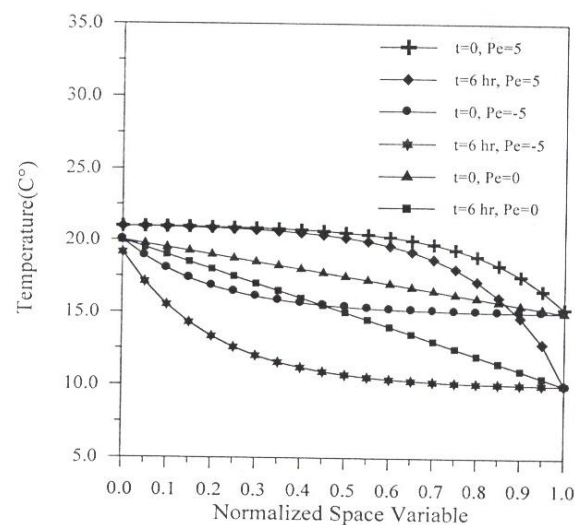


Figure (5) Wall temperature profiles with convection under steady-periodic condition

Figure (6) shows steady-state conductive heat flux profiles across the wall. For three cases: no flow ($Pe = 0$), infiltration flow ($Pe = -5$), and exfiltration flow ($Pe = 5$). The heat flux is constant when no air leaks across the wall. However, heat flux profile changes significantly when air flows across the wall. In the infiltration case, the heat flow is maximum at the inner surface of the wall and decreases to almost zero at the outer surface.

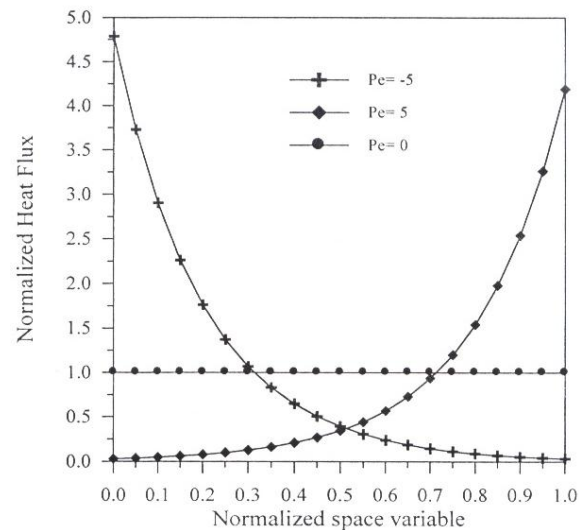


Figure (6) Normalized wall conductive heat flux profiles with convection under steady-state condition

Figure (7) indicates the effect of amount and direction of air flow on the conductive heat flux at the outer and inner surface of the wall. The inner surface conductive heat flux increases with the amount of infiltrating air and decreases with the amount of exfiltrating air. This phenomenon can be explained by the fact that infiltrating air requires heat to increase its temperature. This heat is provided by transmission heat lost at the inner wall surface. On the other hand, exfiltrating air provides heat to the wall resulting an increase of the temperature of the inner wall surface. The temperature gradient (i.e., transmission losses) is then reduced at the inner surface of the wall.

Figure (8) shows the conductive heat flux profiles at the inside wall surface. The conductive heat loss at the inner wall surface is significantly affected by air flowing across wall when warm air leaks to the outside, the conduction heat losses at the inner surface are reduced both in amplitude and mean values. However, when cold air infiltrates through wall, the inner surface loses significantly more heat. Note that a time phase lag exists between the outdoor temperatures (assumed maximum at room). In the no-flow case, this phase lag characterizes the thermal effect of the wall.

Figure (8) indicates that the inner wall response to outdoor conditions lags by about two hours. The time phase lag between temperature and inner wall surface heat losses is minimum for air infiltration (time lag of one half hour) and maximum for air exfiltration (time lag of six hours). Infiltration accelerates the contact between outdoor conditions and indoor, resulting in

a faster wall response to the fluctuations in the outdoor temperature. On the other hand, the warm exfiltrating air delays the wall response to the outdoor temperature.

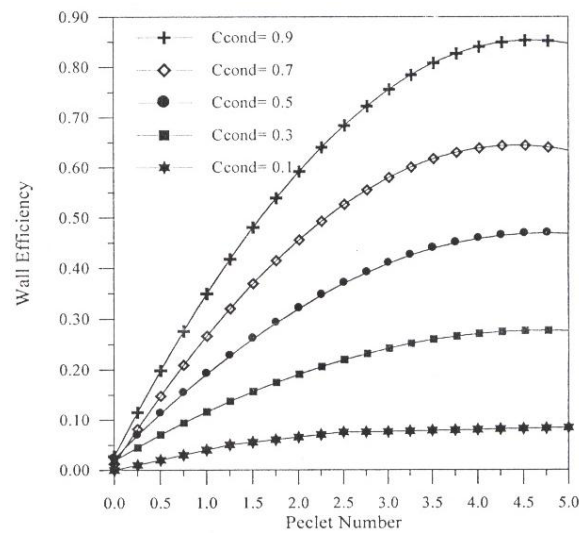


Figure (7) Effect of the peclet number on the steady-state conductive heat flux at the inside and outside wall surface with convection

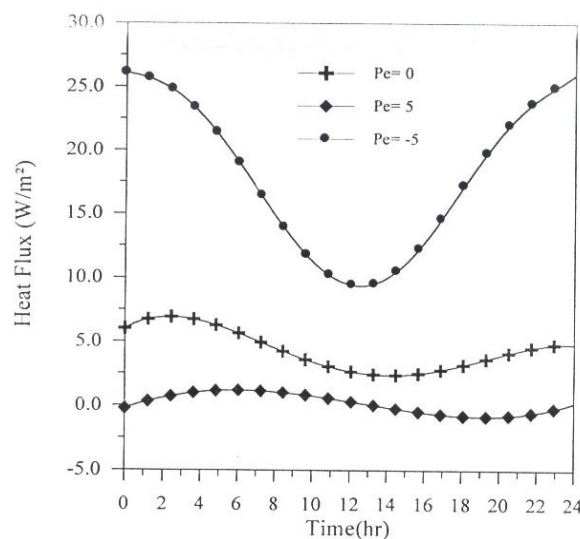


Figure (8) Steady-Periodic conductive heat flux profiles at the inside wall surface with convection

Similar observations can be made for the conductive heat losses at the outer surface of the wall as shown in **Fig.(9)**. In this case; however, infiltrating air reduces the heat losses at the outer wall surface while exfiltrating air increases these losses significantly.

Figure (10) shows the daily heat flux profiles at the inside wall insulation for three different cases (1-pure conduction 2-couples conduction-infiltration, and 3-conduction plus infiltration). Comparison of the heat flux profiles for cases 2 and 3 clearly indicates that thermal coupling reduces the total heating load due to heat conduction and to air leakage through porous walls. Part of the energy needed to warm infiltrating air is directly recovered

from the wall. The wall acts as a heat exchanger between cold infiltrating air and warm porous insulation material. According to **Fig.(8)**, the wall, as a heat exchanger, reduces by almost 20 percent the daily heating load due to conduction and infiltration. These results illustrate clearly the thermal advantage of intentionally circulating air through porous insulation systems to provide ventilation.

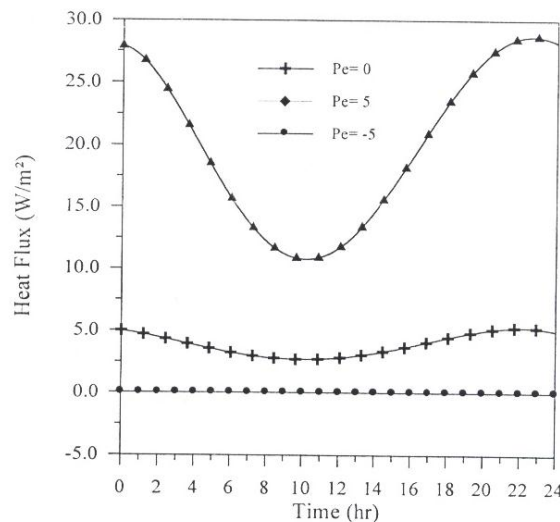


Figure (9) Steady-Periodic conductive heat flux profiles at the outside wall surface with convection

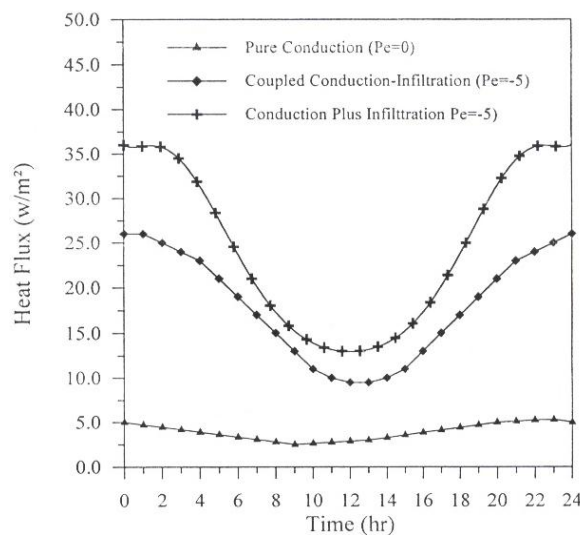


Figure (10) Steady-Periodic heat flux for conductive and infiltration losses at the inside wall surface with convection

Figure (11) illustrates the variation of dynamic wall efficiency as function of the Peclet number (measuring the amount of air flowing through the dynamic wall) for various values the fraction C_{cond} (characterizing the portion of the house thermal load that is due to conductive losses through the dynamic wall).

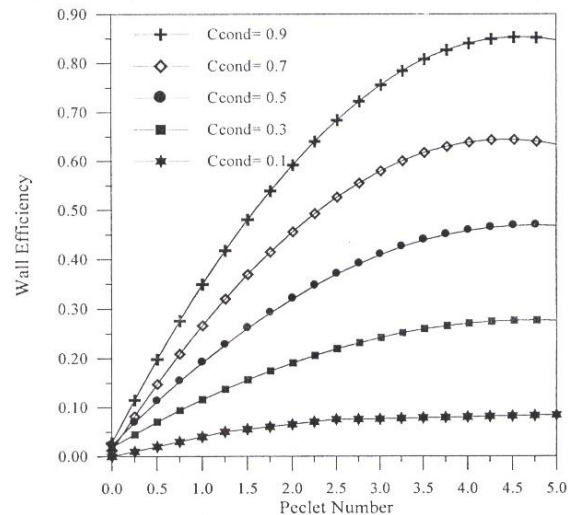


Figure (11) Effect of the peclet number on the dynamic wall efficiency under steady-state condition

4. Conclusions

An analytical model to evaluate the thermal coupling effect of heat conduction and air flow in permeable walls has been developed. The results obtained indicate clearly that air infiltration and exfiltration can affect significantly both the temperature and the heat flux across building walls. In particular, it is found that air infiltration increases the transmission losses at the inner wall surface with a reduced response time lag. Meanwhile air exfiltration decreases conduction heat losses at the inner wall surface but increases the response time lag. A simplified analysis was conducted to evaluate the thermal performance of dynamic insulation systems integrated with a whole building. The analysis indicated that some energy savings can be achieved by the dynamic insulation.

These savings depend mostly on the infiltration flow rate and the building thermal load. The maximum achievable thermal efficiency of a dynamic wall was found to be near 20 percent.

5. References

1. Berlad, A. L., Tutu, N., Yeh, Y., Jaung, R., Krajewski, R., Hoppe, R., and Salzano, F., "Air Intrusion Effects on the Performance of Permeable Insulation Systems", Transaction of the ASME, Vol. 118, 1978, pp. 162-167.
2. Wolf, S., "A Theory for the Effects of Convective Air Flow through Fibrous Thermal Insulation", ASRAE Transactions, Vol. 72, Part 1, 1966, pp.III 2.1-III 2.9.
3. Bankvall, C. G., "Air Movements and Thermal Performance of the Building Envelope", Thermal Insulation: Materials and Systems, F. J. Powell and S. L. Mathews, Eds., ASTM, Philadelphia, PA, 1987, pp. 124-131.

4. Lecompte, J. G. N., ***“The Influence of Natural Convection in an Insulated Cavity on Thermal Performance of a Wall”***, Insulation Materials Testing and Applications, ASTM, FL., 1987.
5. Buchanan, C. R., and Sherman, M. H., ***“A Mathematical Model for Infiltration Heat Recovery”***, Proceedings 21st AIVC Annual Conference, 2000.
6. Powell, F., Krarti, M., and Tuluca, A., ***“Air Movement Influence on the Effective Thermal Resistance of Porous Insulations: A Literature Survey”***, Journal of Thermal Insulation, Vol. 12, 1989, pp. 239-251.
7. Kohonen, R., Ojanen, T., and Virtanen, M., ***“Thermal Coupling of Leakage Flows and Heating Load of Buildings”***, 8th AIVC Conference, Berlingen, FRG, 1987.
8. Claridge, D. E., and Battacharyya, S., ***“The Measured Impact of Infiltration in a Test Cell”***, Journal of Solar Energy Engineering, Vol. 117, 2002, pp. 167-172.
9. Kohonen, R., and Ojanen, T., ***“Non-Steady State Coupled Diffusion and Convection Heat and Mass Transfer in Porous Media”***, 5th International Conference on Numerical Methods in Thermal Problems, Montreal Canada, 1987.
10. Bailey, N. R., ***“Dynamic Insulation Systems and Energy Conservation in Buildings”***, ASHRAE Transactions, Vol. 91, Part I, 1985, pp. 447-466.
11. Vafai, K., and Sozen, M., ***“Analysis of Energy and Momentum Transport for Fluid Flow through a Porous Bed”***, ASME Journal of Heat Transfer, Vol. 112, 1990, pp. 690-699.
12. Timusk, J., ***“Design, Construction and Performance of a Dynamic Wall House”***, Proceedings, Ventilation Technology, Research and Application, 8th AIVC Conference, AIVC Centre, 1987.
13. Brunsell, J. T., ***“The Performance of Dynamic Insulation in Two Residential Building”***, Proceeding 15th AIVC Conference: The Role of Ventilation, Air Infiltration and Ventilation Center, Coventry U.K, 2003, pp. 285-288.